Polyhedron 62 (2013) 169–178

Contents lists available at SciVerse ScienceDirect

Polyhedron

journal homepage: www.elsevier.com/locate/poly

Facile synthesis of platinum based heterobimetallic carbonyl clusters from bis(1-alkenyl)Pt(II) precursors

Chinduluri Sravani [a], Sadhana Venkatesh [a], Akella Sivaramakrishna [a,*], Kari Vijayakrishna [a], Hadley S. Clayton [b], John R. Moss [c], Viktor Moberg [c], Hong Su [c]

[a] Chemistry Division, School of Advanced Sciences, VIT University, Vellore 632 014, Tamil Nadu, India
[b] Department of Chemistry, University of South Africa, Pretoria, South Africa
[c] Department of Chemistry, University of Cape Town, Rondebosch 7701, Cape Town, South Africa

ARTICLE INFO

Article history:
Received 17 May 2013
Accepted 4 June 2013
Available online 27 June 2013

Keywords:
Platinum–ruthenium mixed cluster
Platinum-alkenyl complex
Synthesis
Reactivity
Structure

ABSTRACT

A new route for the high yield synthesis of platinum containing mixed bimetallic carbonyl clusters of the type $[PtRu_2(CO)_8L_2]$ (where L_2 = dppe, 1,2-bis(diphenylphosphino)ethane or dppp, 1,3-bis(diphenylphosphino)propane; L = PPh_3) by the reaction of platinum-alkenyl $[PtL_2(1\text{-alkenyl})_2]$ precursors with $[Ru_3(CO)_{12}]$ is reported. An unexpected multinuclear mixed cluster, $[PtRu_4(CO)_{13}(\mu_4\text{-}PCH_2CH_2CH_2PPh_2)]$, obtained under prolonged refluxing conditions was also isolated. All the products were isolated and characterized by various spectroscopic and analytical techniques. In solution, the complex $[PtRu_2(CO)_8(PPh_3)_2]$ gives $[Pt_2Ru(\text{-}CO)_3(CO)_2(PPh_3)_3]$ and $Ru_3(CO)_{11}(PPh_3)$. The structures and relative energies of the intermediates and transition states in the proposed reaction mechanism for the {$PtRu_2$} clusters have been investigated using density functional theory.

1. Introduction

The chemistry of mixed-metal clusters has received much attention because of their interesting structural features, synergistic effects and catalytic potential [1]. The design of nanoparticle catalysts has been imperative in the initial synthesis of bimetallic clusters and hence the need for reliable and efficient synthetic routes is inevitable [2]. Among them, platinum based heterobimetallic carbonyl clusters are very well known [3]. The main methods used for the synthesis of these Pt based heterobimetallic clusters are (i) reaction of either $Pt(0)L_4$ or $L_2Pt(II)Cl_2$ (L = PPh_3 and other ligands) with various $M_3(CO)_{12}$ clusters or their derivatives (where M = Os or Ru) and (ii) by splitting larger clusters into smaller ones and, (iii) aggregating small clusters into multinuclear heterobimetallic clusters. It is known that these carbonyl clusters react by; (i) cleavage of bonds in larger clusters to form smaller clusters, (ii) condensation of two mixed metal clusters, thus forming high nuclear cluster compounds, (iii) ligand substitution and/or addition (ligands include phosphines, diphosphines, thioethers, carbonyls, 1,5-cyclooctadiene (COD), alkynyls, vinylidenes and mononuclear systems), (iv) the reaction with different substrates, and (v) intramolecular M–M rearrangement of ligands and/or dynamical fluxionality within clusters [3].

The reaction between $[Ru_3(CO)_{11}(CNBu^t)]$ and $[Pt(\eta\text{-}C_2H_4)(PPh_3)_2]$ at −30 °C afforded $[Ru_2Pt(CO)_7(PPh_3)_3]$, $[RuPt_2(CO)_5(PPh_3)_3]$, $[RuPt_2(CO)_6(CNBu^t)(PPh_3)]$, $[Ru_2Pt_2(CO)_9(CNBu^t)(PPh_3)]$ and the hexanuclear complexes $[Ru_2Pt_4(CO)_{5-n}(CNBu^t)(PPh_3)_{4+n}]$, where $n = 0$ and 1 [4]. The reaction of $Pt[COD]_2$ with $Ru(CO)_5$ at 25 °C produced the hexanuclear metal complex, $[PtRu_2(CO)_9]_2$, which consists of an open cluster containing two ruthenium atoms bonded to two platinum atoms, followed by two additional ruthenium atoms. This dimeric compound has also been used to synthesize other known trinuclear Pt–Ru cluster derivatives with various ligand systems [5], but in low yields. The rearrangement of the spiked triangular cluster $[Ru_3Pt(\text{-}H)(_4\text{-}\eta^2\text{-}CCBu^t)(CO)_9(dppe)]$ in solution into the butterfly cluster $[Ru_3Pt(_4\text{-}\eta^2\text{-}C{=}CHBu^t)(CO)_9(dppe)]$ has been reported [6]. The cluster complex $PtRu_5(CO)_{15}(PMe_2Ph)(\mu_6\text{-}C)$ has also been shown to exhibit a facile intramolecular exchange of the phosphine ligand between the platinum and a ruthenium atom. The reaction of $Pt_2M_4(CO)_{18}$ (where M = Ru or Os) with cyclooctadiene in the presence of UV irradiation resulted the formation of different mixed metal clusters [7]. The synthesis of new Sn and Ge containing $PtRu_5$ clusters was also achieved by the reaction of $PtRu_5(CO)_{14}(PBu_3^t)(\mu\text{-}H)_2(\mu_6\text{-}C)$ with $HGePh_3$ and $HSnPh_3$ under reflux Eqs. (2) and (3) [8]. They are widely used in the petroleum industry [9] as precursors for catalytically active metal nanoparticles and in fuel cells [10]. Ruthenium based catalysts modified with Group 10 metals, e.g. Pt and Pd, were found to be exceptionally active and selective in a number of industrially important hydrogenation processes [11].

---

* Corresponding author. Tel.: +91 4162202351; fax: +91 4162243092.
E-mail address: asrkrishna@rediffmail.com (A. Sivaramakrishna).

0277-5387/$ - see front matter © 2013 Elsevier Ltd. All rights reserved.
http://dx.doi.org/10.1016/j.poly.2013.06.011

The present paper describes a facile and novel route for the synthesis of mixed trinuclear metal carbonyl clusters of the type $[PtRu_2(CO)_8L_2]$ (L = PPh_3; L_2 = dppe or dppp) using the reaction of $[Ru_3(CO)_{12}]$ with $[PtL_2(1\text{-alkenyl})_2]$, which have exhibited a rich chemistry in the recent past [12] (Scheme 1).

2. Experimental part

2.1. Materials and methods

All reactions and manipulations were carried out under an inert atmosphere of dry nitrogen using standard Schlenk and vacuum-line techniques. $[Pt(COD)Cl_2]$ [13] (COD = 1,5-cyclooctadiene), $[Pt(dppp)Cl_2]$ (dppp = 1,3-bis(diphenylphosphino)propane) (**1a**), $[Pt(dppe)Cl_2]$ (dppe = 1,2-bis(diphenylphosphino)ethane) (**1b**), $[Pt(PPh_3)_2Cl_2]$ (PPh_3 = triphenylphosphine) (**1c**), $[Pt(dppm)Cl_2]$ (dppm = 1,1-(bis(diphenylphosphino)methane) (**1d**), $[Pt(dppp)\{(CH_2)_3CH=CH_2\}_2]$ (**2**) [8], $[Pt(dppe)\{(CH_2)_3CH=CH_2\}_2]$ (**3**) [9], $[Pt(PPh_3)_2\{(CH_2)_3CH=CH_2\}_2]$ (**4**) [9] and $[Pt(dppm)\{(CH_2)_3CH=CH_2\}_2]$ (**8**) [12] were prepared as previously described. $[Pt(COD)Me_2]$ (Sigma–Aldrich) was purchased and used as received. $[Pt(dppe)Me_2]$ was prepared from $[Pt(COD)Me_2]$ by treatment with dppe in CH_2Cl_2. The solvents were purchased from commercially available sources and distilled from dark purple solutions of sodium/benzophenone ketyl prior to use.

2.1.1. Nuclear magnetic resonance spectroscopy

^1H and ^{31}P NMR spectra were recorded on a Bruker DXM-400 spectrometer. All ^1H chemical shifts are reported referenced to the residual proton resonance in the deuterated solvent used. All ^{31}P chemical shifts are ^1H decoupled and referenced to an 85% phosphoric acid external peak at 0 ppm.

2.1.2. Elemental analysis

Micro analyses were conducted with a Thermo Flash 1112 Series CHNS–O analyzer instrument.

2.1.3. GC–MS analysis

GC analyses were carried out using a Varian 3900 gas chromatograph equipped with an FID and a 30 m × 0.32 mm CP-Wax 52 CB column (0.25 μm film thickness). The carrier gas was helium at 5.0 psi. The oven was programmed to hold the temperature at 32 °C for 4 min and then to ramp to 200 °C at 10 °C/min and hold for 5 min. GC–MS analyses for peak identification were performed using an Agilent 5973 gas chromatograph equipped with MSD and a 60 m × 0.25 mm Rtx-1 column (0.5 μm film thickness). The carrier gas was helium at 0.9 mL/min. The oven was programmed to hold the temperature at 50 °C for 2 min and then ramp to 250 °C at 10 °C/min and hold for 8 min.

2.1.4. Infrared spectroscopy

Infrared spectra were recorded on a Perkin-Elmer FT-IR spectrometer.

2.1.5. UV irradiation studies

Irradiations were carried out with an Englehard Hanovia Lamp (125 W) at a distance of 16 cm from the reaction vessel.

2.1.6. Mass spectrometry

Mass spectral data was obtained using a VG70SE with 8 kV acceleration and the FAB gun was an Iontech Saddlefield, using xenon gas and operating at 8 kV. All matrices were made with 3-nba.

2.1.7. Crystallographic data for the compound $[PtRu_4(CO)_{13}(\mu_4\text{-}PCH_2CH_2CH_2PPh_2)]$ (**5a**)

X-ray single crystal intensity data were collected on a Nonius Kappa-CCD diffractometer using graphite monochromated Mo K radiation. The temperature was controlled by an Oxford Cryostream cooling system (Oxford Cryostat). The strategy for the data collection was evaluated using the Bruker Nonius "Collect" program. Data were scaled and reduced using DENZO-SMN software [14].

The structure was solved by direct methods and refined employing full-matrix least-squares with the program SHELXL-97

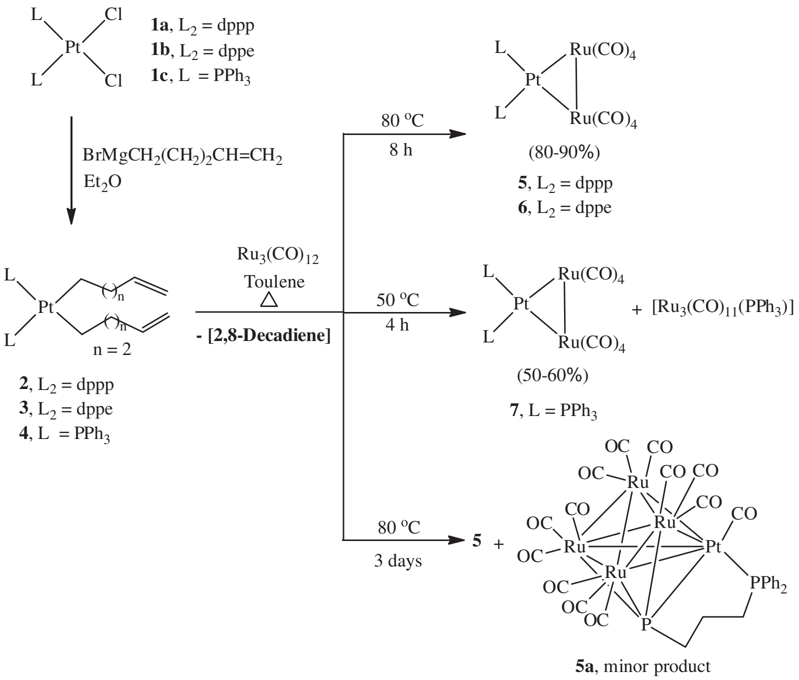

Scheme 1.

[15] refining on F^2. Packing diagrams were produced using the program PovRay and graphic interface X-seed [16]. All non-H atoms were refined anisotropically. All the hydrogen atoms, except the amino hydrogens H1A and H1B, were included in idealized positions in a riding model with U_{iso} set at 1.2 or 1.5 times those of the parent atoms. H1A and H1B were located by difference Fourier methods and refined independently with a simple bond length constraint. The structure was refined successfully with $R = 0.0238$.

(CCDC number 900110) [16]: $C_{28}H_{16}O_{13}P_2PtRu_4$, M.w.t = 1221.72 g mol^{-1}, monoclinic, space group $P2_1/c$, $a = 9.4382(2)$ Å, $b = 11.4153(3)$ Å, $c = 31.4264(6)$ Å, = 90°, = 95.801(2)°, = 90°, $V = 3368.54(13)$ Å^3, $Z = 4$, $_{calcd}$ = 2.409 Mg/m^3, $T = 173(2)$ K, = 6.048 mm^{-1}, $F(000) = 2288$, crystal size 0.15 × 0.14 × 0.14 mm^3. Intensity data were collected with a Nonius Kappa CCD diffractometer. 94236 reflections, 6393 independent ($R_{int} = 0.0519$), multi-scan absorption correction (SADABS), structure solution using direct methods (SHELXS-97), structure refinement on F^2 using full-matrix least-squares procedures (SHELXL-97), $R_1 = 0.0238$ $[I > 2(I)]$, $wR_2 = 0.0449$ (all data), GOF = 1.194, max./min. residual electron density = 0.929/−0.686 e Å^{-3} [17].[1]

2.1.8. Crystallographic data for the compound $[Pt_2Ru(CO)_2(\mu\text{-}CO)_3(PPh_3)_3]$ (**13**)

(CCDC number 671765) [14]: $C_{59}H_{45}P_3Ru_1Pt_2O_5$, M.w.t = 1418 g mol^{-1}, triclinic, space group $P\bar{1}$, $a = 12.5217(1)$ Å, $b = 13.4675(1)$ Å, $c = 15.6595(1)$ Å, = 85.026(1)°, = 77.121(1)°, = 72.026(1)°, $V = 2448.23(3)$ Å^3, $Z = 2$, $_{calcd}$ = 1.924 Mg/m^3, $T = 113$ (2) K, = 6.155 mm^{-1}, $F(000) = 1368$, 5.70 < 2 < 51.83, (Mo k) = 0.71073 Å, crystal size 0.14 × 0.18 × 0.18 mm^3. Intensity data were collected [17] with a Nonius Kappa CCD diffractometer. 61 236 reflections, 9276 independent ($R_{int} = 0.0315$), multi-scan absorption correction (SADABS), structure solution using direct methods (SHELXS-97), structure refinement on F^2 using full-matrix least-squares procedures (SHELXL-97), $R_1 = 0.0195$ $[I > 2(I)]$, $wR_2 = 0.0420$ (all data), GOF = 1.102, max./min. residual electron density = 0.693/−0.583 e Å^{-3}.

2.1.9. Crystallographic data for the compound $PtRu_2(CO)_6(\mu\text{-}dppm)_2]$ (**14**)

(CCDC number 670301) [14]: $C_{56}H_{44}O_6P_4PtRu_2 \cdot 2(C_6H_6)$, M.w.t = 1490.24 g mol^{-1}, monoclinic, space group $P2_1/c$, $a = 15.8482(10)$ Å, $b = 19.7322(12)$ Å, $c = 18.9112(12)$ Å, = 94.072(3)°, $V = 5899.0(6)$ Å^{-3}, $Z = 4$, $_{calcd}$ = 1.678 Mg/m^3, $T = 100(2)$ K, $F(000) = 2952$, 3.30 < 2 < 105.98, (Mo k) = 0.71073 Å, crystal size 0.33 × 0.30 × 0.19 mm^3. Intensity data were collected [14] with a Bruker KAPPA APEX II diffractometer. 258672 reflections, independent reflections 66042 [$R_{int} = 0.0657$], multi-scan absorption correction (SADABS), structure solution using direct methods (SHELXS-97), structure refinement on F^2 using full-matrix least-squares procedures (SHELXL-97), $R_1 = 0.0395$ $[I > 2(I)]$, $wR_2 = 0.0629$ (36020 reflections), GOF = 1.225 max./min. transmission = 0.5965/0.4343 e Å^{-3}.

2.1.10. Computational details

All calculations were carried out using the DMol^3 density functional theory (DFT) code as implemented in the Accelrys Material Studio® 5.0 software package [17]. The non-local generalized gradient approximation (GGA) using the PW91 exchange–correlation functional was used for geometry optimizations in all cases [18]. A double numeric, polarized split valence (DNP) basis set was used in this study with a DFT semi-core pseudo potential to account for relativistic effects in Ru and Pt. The size of the DNP basis set is comparable to GAUSSIAN 6-31G**, but the DNP is more accurate than the GAUSSIAN basis set of the same size [19]. This combination of basis set and functional has been used successfully in previous studies of Pt and Ru complexes [20,21] Geometry optimizations were performed without any symmetry constraints and the relative energies were compared taking into account the total number of molecules present. The convergence criteria for these optimizations consisted of the following threshold values: 1×10^{-5} Ha for energy; 0.002 Ha Å^{-1} for gradient and 0.005 Å for displacement convergence, while a self-consistent field density convergence threshold of 1×10^{-6} Ha was specified. All optimized geometries were subjected to a full frequency analysis at the same level of theory (GGA/PW91/DNP) to verify the nature of the stationary points. Equilibrium geometries were characterized by the absence of imaginary frequencies.

The phenyl substituents on the bis-phosphino ligand contain a large number of atoms which contribute little to the electronic structure of these complexes, and consequently they were replaced by H atoms in the calculations to reduce the computational demands of the system.

2.2. Synthetic methodology

2.2.1. Preparation of $[PtRu_2(CO)_8(dppp)]$ (**5**)

2 (256 mg, 0.3433 mmol) and $[Ru_3(CO)_{12}]$ (220 mg, 0.3441 mmol) were dissolved in 10 mL of toluene. The reaction mixture was then heated to 80 °C in a closed flask under reduced pressure for 8 h. A dark colored solution was formed. The reaction was monitored by ^{31}P NMR until the completion of the reaction. All the volatiles were removed by a high vacuum pump and the residue was dissolved in 5 mL of CH_2Cl_2 and added to the top of a silica gel column. An orange red band was collected by eluting with a solvent mixture of 4:1 CH_2Cl_2: *n*-hexane. The product was obtained as a bright orange red solid (**5**). Yield: 319 mg (90%). M.p.: 166–169 °C (dec.). *Anal.* Calc. for $C_{35}H_{26}O_8P_2PtRu_2$ (1034.88): C, 40.67; H, 2.54. Found: C, 40.48; H, 2.92%. IR (ν_{CO}/cm^{-1}) in CH_2Cl_2: 2066 m, 2023vs, 1997sh, 1983s, 1960sh. ^1H NMR ($CDCl_3$) δ: 6.85–7.73 (m, 20H, Ph), 1.84–2.40 (m, 6H, P–CH_2); ^{31}P NMR ($CDCl_3$) δ: 8.35 (J_{Pt-P} = 3079 Hz). Mass Data, *m*/*z*: 1034.9 [M]$^+$; 607.1 [(dppp)Pt]$^+$.

2.2.2. Preparation of $[PtRu_2(CO)_8(dppe)]$ (**6**)

3 (225 mg, 0.3075 mmol) and $[Ru_3(CO)_{12}]$ (200 mg, 0.3128 mmol) were dissolved in 10 mL of toluene and then the mixture was heated to 80 °C in a closed flask under reduced pressure for 8 h. A similar work-up procedure was used as mentioned above to isolate an orange red solid (**6**). Yield: 244 mg (78%). M.p.: 85–90 °C (dec.). *Anal.* Calc. for $C_{34}H_{24}O_8P_2PtRu_2$ (1019.72): C, 40.05; H, 2.37. Found: C, 40.79; H, 2.44. IR (ν_{CO}/cm^{-1}) in CH_2Cl_2: 2063s, 2025s, 1978br, 1953m. ^1H NMR ($CDCl_3$) δ: 7.34–7.98 (m, 20H, Ph), 1.92–2.20 (m, 4H, P–CH_2); ^{31}P {^1H} NMR ($CDCl_3$) δ: 61.3 (J_{Pt-P} = 3117 Hz). Mass Data, *m*/*z*: 1019.7 [M]$^+$, 593.1 [Pt(dppe)]$^+$.

2.2.3. Preparation of $[PtRu_4(CO)_{13}(\mu_4\text{-}PCH_2CH_2CH_2PPh_2)]$ (**5a**)

2 (186 mg, 0.2494 mmol) and $[Ru_3(CO)_{12}]$ (164 mg, 0.2565 mmol) were dissolved in 10 mL of toluene. The reaction mixture was then heated to 80 °C in a closed flask under reduced pressure for 3 days. An intense red colored solution was formed. The ^{31}P NMR spectrum of the crude reaction mixture indicated the formation of **5** as a major product at 8.35 ppm (J_{Pt-P} = 3079 Hz) and a new doublet at 13.2 ppm (J_{Pt-P} = 3126 Hz). All the volatiles were removed by a high vacuum pump and the residue was dissolved in 5 mL of CH_2Cl_2 and added to the top of a silica gel column. An orange red band was collected by eluting with a solvent mixture of 4:1 CH_2Cl_2:*n*-hexane. The major product, a bright orange red solid (**5**), was obtained in 72% yield and isolated as mentioned above. Then using CH_2Cl_2:*n*-hexane (10:1) as the eluant, an intense green

---

[1] Crystallographic data have been deposited at the CCDC, 12 Union Road, Cambridge CB2 1EZ, UK and copies can be obtained on request, free of charge, by quoting the publication citation and the deposition number 670301.

band was separated, and it was found to be a stable and new heterobimetallic carbonyl cluster containing a {$PtRu_4$} template (**5a**) in 2% yield. M.p.: 206–208 °C (dec.). *Anal.* Calc. for $C_{28}H_{16}O_{13}P_2PtRu_4$ (1221.73): C, 27.53; H, 1.32. Found: C, 27.48; H, 1.30%. IR (ν_{CO}/cm^{-1}) in CH_2Cl_2: 2061m, 2044vs, 2031m, 2013s; ^{1}H NMR ($CDCl_3$) δ: 6.78–7.64 (m, 10H, Ph), 1.82–2.32 (m, 6H, P-CH_2); ^{31}P {^{1}H} NMR ($CDCl_3$) δ: 13.2 (d, $^2J_{P-P}$ = 14 Hz, $^1J_{Pt-P}$ = 3126 Hz, Pt–P), 408.0 (d, $^2J_{P-P}$ = 14 Hz, $^1J_{Pt-P}$ = 864 Hz, Pt–P).

2.2.4. Preparation of [$PtRu_2(CO)_8(PPh_3)_2$] (7)

4 (266 mg, 0.31 mmol) and [$Ru_3(CO)_{12}$] (202 mg, 0.316 mmol) were dissolved in 10 mL of toluene and then the mixture was heated to 50 °C in a closed flask under reduced pressure for 4 h. A similar work-up procedure was used as mentioned above to isolate an orange red solid (**7**). Yield: 195 mg (55%). M.p.: 188–192 °C (dec.). *Anal.* Calc. for $C_{44}H_{30}O_8P_2PtRu_2$ (1145.88): C, 46.12; H, 2.64. Found: C, 45.89; H, 2.72%. IR (ν_{CO}/cm^{-1}) in CH_2Cl_2: 2045w, 2028s, 2013w. ^{1}H NMR ($CDCl_3$) δ: 7.36–8.43 (m, 30H, Ph); ^{31}P NMR ($CDCl_3$) δ: 35.2 (J_{Pt-P} = 4577 Hz). Mass Data, *m*/*z*: 1146.92 [M]$^+$, 719.15 [$(PPh_3)_2Pt$]$^+$.

2.2.5. Preparation of [$Pt_2Ru(CO)_2(\mu\text{-}CO)_3(PPh_3)_3$] (13)

7 (120 mg, 0.1046 mmol) was taken in 5 mL of CH_2Cl_2 and the solution was irradiated with UV light in a closed flask under reduced pressure for 18 h at room temperature. The solvent was removed under vacuum and then the residue was chromatographed on a silica gel column using CH_2Cl_2 as the eluent. A red band was isolated and dried under vacuum for a few hours. The residue was recrystallized from CH_2Cl_2:*n*-hexane (1:3) to obtain single crystals. Yield: 27 mg (36%). M.p.: 225–226 °C (dec.). *Anal.* Calc. for $C_{44}H_{30}O_8P_2Pt_2Ru$ (1418.08): C, 49.97; H, 3.20. Found: C, 49.89; H, 3.52%. IR (ν_{CO}/cm^{-1}) in CH_2Cl_2: 2020s, 1947s, 1852w, 1791vs. ^{1}H NMR ($CDCl_3$) δ: 7.46–8.69 (m, 30H, Ph); ^{31}P NMR ($CDCl_3$) δ: 35.2 (J_{Pt-P} = 4577 Hz) (Pt–P), 26.6 (Ru–P). Mass Data, *m*/*z*: 1417.8 [M]$^+$ and loss of CO and PPh_3 groups at 1334, 1306, 896, 868 and comparison with the literature values [25].

2.2.6. Preparation of [$PtRu_2(CO)_6(\mu\text{-dppm})_2$] (14)

8 (322 mg, 0.44866 mmol) and [$Ru_3(CO)_{12}$] (292 mg, 0.4567 mmol) were suspended in 5 mL of toluene and the mixture was heated at 80 °C for 8 h. The solvent from the resulting dark orange red solution was removed under vacuum and then the residue was chromatographed on a silica gel column using CH_2Cl_2 as the eluent. The orange red band was isolated, and dried under vacuum after removing the solvent. The solid residue was recrystallized from CH_2Cl_2/*n*-hexane to obtain single crystals of **14**. Yield: 160 mg (26%). M.p.: 236–238 °C (dec.). *Anal.* Calc. for $C_{56}H_{44}O_6P_4PtRu_2$ (1411.17): C, 50.41; H, 3.32. Found: C, 50.45; H, 3.42. IR (ν_{CO}/cm^{-1}) in CH_2Cl_2: 2007s, 1960s, 1940sh, 1924s, 1893s, 1878b; ^{1}H NMR ($CDCl_3$) δ: 4.5 (m, 4H, P–CH_2), 6.95–7.98 (m, 40H, Ph); ^{31}P {^{1}H} NMR ($CDCl_3$) δ: 16.4 (d, $^2J_{P-P}$ = 48 Hz, Ru–P), 8.0 (d, $^2J_{P-P}$ = 48 Hz, $^1J_{Pt-P}$ = 3130 Hz, Pt–P).

3. Results and discussion

3.1. Synthesis and characterization

Most of the reported methods for synthesizing platinum containing bi- and polynuclear metal carbonyl cluster complexes are based on the reactions of the appropriate metal–carbonyls with Pt(0) species as precursors [22]. In addition, a secondary method for the synthesis of heteronuclear multimetallic clusters of platinum containing cobalt or molybdenum has been reported using the carbonylmetallate salts Na[$Co(CO)_4$] or Na[η-C_5H_5)Mo(CO)$_3$] with *cis*- or *trans*-$PtCl_2(PPh_3)_2$ [23]. The groups of Stone and Woodward, and recently Adams, have extensively studied the synthesis as well as novel reactivity patterns of platinum based bi- and trimetallic carbonyl clusters [24–26]. Usually the literature methods for the carbonyl cluster synthesis indicate a mixture of clusters and low yields. To the best of our knowledge, there is no direct method available for the synthesis of trinuclear heterobimetallic clusters selectively.

The bis(1-alkenyl)platinum(II) complexes **2**–**4** were prepared by the reactions of **1a-c** with the appropriate Grignard reagents, as shown in Scheme 1. Investigations on the reactions of **2**–**4** with ruthenium-carbonyls were carried out with the aim of forming mixed metal complexes via olefin coordination to ruthenium. In contrast, the formation of trinuclear cluster compounds with a {$PtRu_2$} core, [$L_2PtRu_2(CO)_8$] (where L_2 = dppp (**2**) or dppe (**3**); L = PPh_3 (**4**)) (Scheme 1), by the subsequent elimination of the organic fragment was observed. The products **5**–**7** were identified by IR, ^{1}H and ^{31}P NMR spectroscopy, mass spectrometry and elemental analysis. The data for the compounds **6** [5] and **13** [4] are consistent with the literature reports and the yields were found to be superior to the reported methods [5,27].

The formation of mixed platinum bimetallic trinuclear clusters was observed when reacted with [$Ru_3(CO)_{12}$]. It is noteworthy that no similar clusters were observed with the dppm ligand (**8**). Reactions of **2**–**4** with [$Co_2(CO)_8$] yielded known trinuclear and tetranuclear carbonyl clusters of the type [$Co_2Pt(\mu\text{-}CO)(CO)_6(L_2)$] and [$Co_2Pt_2(\mu\text{-}CO)_3(CO)_5(PPh_3)_2$] [28]. It is interesting to note that no cluster formation was observed when reacting **2** with other metal carbonyls, including [$W(CO)_6$] and [$Mo(CO)_6$], under identical reaction conditions.

Attempts were made to observe the formation of intermediate complexes in the overall reaction of **2** and **3** separately with [$Ru_3(CO)_{12}$] in toluene at 80 °C by monitoring the samples with IR and ^{1}H and ^{31}P NMR spectroscopy at 30 min intervals. The ^{1}H decoupled ^{31}P NMR chemical shift of **2** at δ 3.48 (J_{Pt-P} = 1645 Hz)) was changed to δ 8.9 (J_{Pt-P} = 3079 Hz) (**5**). In a similar way, **3** (δ 46.4 (J_{Pt-P} = 1619 Hz)) forms **6** (δ 61.2 (J_{Pt-P} = 3157 Hz)). It is predicted that $Ru_3(CO)_{12}$ at 80 °C can form the very reactive intermediate **9** along with coordinatively unsaturated $Ru(CO)_4$ species in the presence of **5** or **6** [29]. Then the corresponding allylic hydride species (**10**) can result from **9**, and this can be envisaged based on literature reports [30] (i.e. the isomerization of a terminal olefin to an internal olefin is consistent with the allylic metal hydride intermediate pathway (**10**)). This is also in accordance with a similar reported mechanism on the selective isomerization of 1-alkenes to the corresponding 2-alkenes by various metal–carbonyl cluster compounds, particularly with [$Ru_3(CO)_{12}$] [31]. The progress of the reaction for **3** → **6** was monitored by ^{31}P NMR spectroscopy, as shown in Scheme 2. The bis(2-alkenyl)Pt(II) species were considered to be the intermediates that were identified by ^{31}P NMR spectroscopy. The broad signals observed in the range δ 46.3–46.8 for **6** reveal the presence of three different isomers, *E*/*E*, *E*/*Z*, *Z*/*Z* (**11**), as shown in Scheme 2. This is validated by our earlier observations of the quantitative isomerization of bis(1-alkenyl)Pt(II) to bis(2-alkenyl)Pt(II) complexes under similar conditions [10]. Fig. 1 illustrates the formation of various species during the reaction of **3** with $Ru_3(CO)_{12}$ at 80 °C in toluene after different time intervals, and this directly supports the proposed isomerized species **11** (Scheme 2). When the infra red spectrum of $Ru_3(CO)_{12}$ was compared with the crude reaction mixture, as well as the product $(L_2)PtRu_2(CO)_8$ (where L_2 = dppe or dppp), significant changes in the region from 2122 to 1977 cm^{-1} were observed.[2] They have been attributed to the formation of interme-

---

[2] See supporting information Fig. 7 for the corresponding FT-IR data.

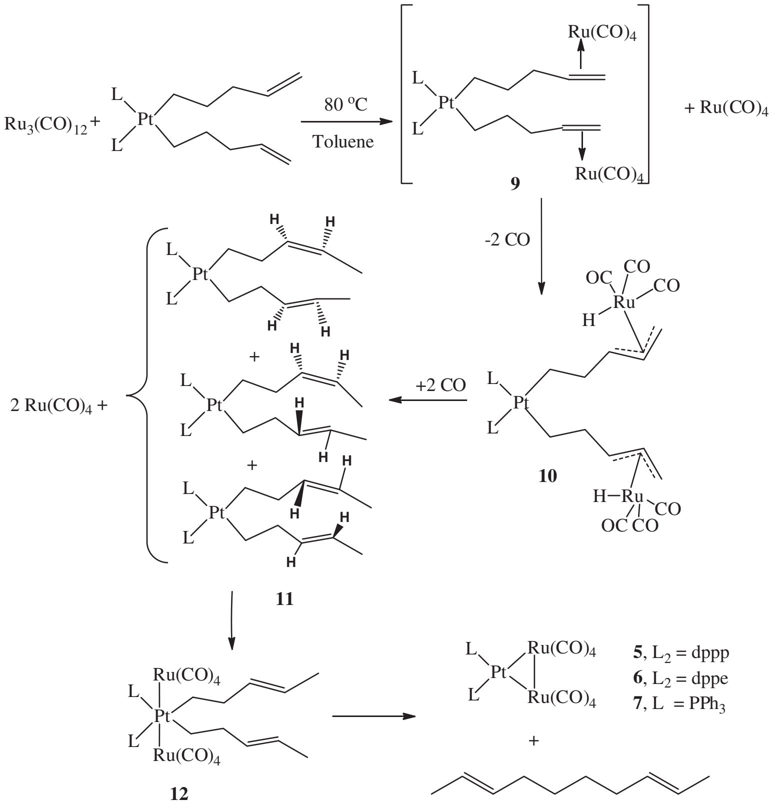

Scheme 2. Proposed reaction mechanism for the formation of the trinuclear {$PtRu_2$} carbonyl clusters.

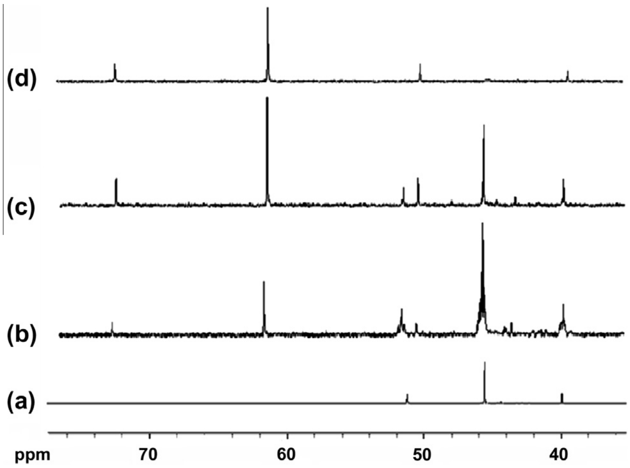

Fig. 1. Proton decoupled ^{31}P NMR spectra recorded during the reaction of **3** with $Ru_3(CO)_{12}$ at 80 °C in toluene to obtain **6**: (a) before heating the reaction mixture; (b) after 1 h heating; (c) after 10 h heating; (d) after 12 h heating.

diates **10**, **11** and **12** (see Scheme 2). No spectroscopic evidences were obtained for the identification of compounds **9** and **12**.

To investigate this further, the reaction between **3** and $Ru_3(CO)_{12}$ in toluene-d_8 was followed *in situ* at 100 °C using NMR spectroscopy. The ^1H NMR spectra revealed a signal at δ −15.2, which was attributed to Ru–H and a broad multiplet at δ 2.2–2.5, indicating the presence of an allylic ruthenium hydride intermediate (**10**) that forms the bis(2-alkenyl)Pt(II) species (**11**). Further, these isomerized species (**11**) undergo an oxidative addition reaction with [$Ru(CO)_4$] fragments to yield unstable heaxacoordinate Pt(IV) species (**12**). The identification of long chain dienes by GC–MS confirms the reductive elimination pathway, which further supports the intermediacy of the hexacoordinate Pt(IV) species. In all the reactions, the organic product distribution reveals the presence of 2,8-decadiene (98%), traces of *n*-pentane (0.5%), 2-pentene (0.5%, a mixture of *cis*- and *trans*- isomers) and 1,4-pentadiene (1.0%).

In contrast, the reaction with prolonged heating gave smaller amounts of **5a** and afforded **5** as the major product. The green product **5a**, formed unexpectedly, was isolated by column chromatography in very low yields. As the formation of multi nuclear clusters is known by different routes [5b], the structural characterization of **5a** showed a novel cluster with a bridging diphosphine. Spectroscopically, **5a** is characterized by its infrared spectrum and by proton decoupled ^{31}P NMR resonances at low field. The formation of **5a** clearly results from cluster aggregation to form the mixed Pt–Ru cluster $Ru_4(CO)_{13}Pt(CO)(\mu_4\text{-}PCH_2CH_2CH_2PPh_2)$ (**5a**) (Scheme 1).

In order to try and shed more light on the mechanism of the reaction, similar experiments were carried out using other organoplatinum complexes, bearing either different ligand systems or different alkyl groups. Thus, attempts to react [$Ru_3(CO)_{12}$] with [$Pt(COD)Me_2$] and [$Pt(dppe)Me_2$] under similar reaction conditions did not yield the clusters **5–7**. It appears that the pendant olefinic group plays a key role in activating the metal carbonyl precursors to produce these heterobimetallic cluster compounds.

An ORTEP diagram of compound **5a** is shown in Fig. 2. The ruthenium atoms are arranged in a square-based pyramidal geometry with the phosphorus atom of the phosphinidene ligand occupying one of the basal sites. The square base is capped with the platinum center, resulting in an octahedral arrangement of the six core cluster atoms. The platinum center is bound by one carbonyl and one diphenylphosphino end of the dppp ligand, while each ruthenium center has three terminal carbonyl ligands.

The phosphorus atom of second end of dephenylated dppp ligand ($\mu_4\text{-}PCH_2CH_2PPh_2$) lies on the Ru(1), Ru(3), Ru(4), Pt(1) atoms by forming a six membered ring with platinum, resulting in an

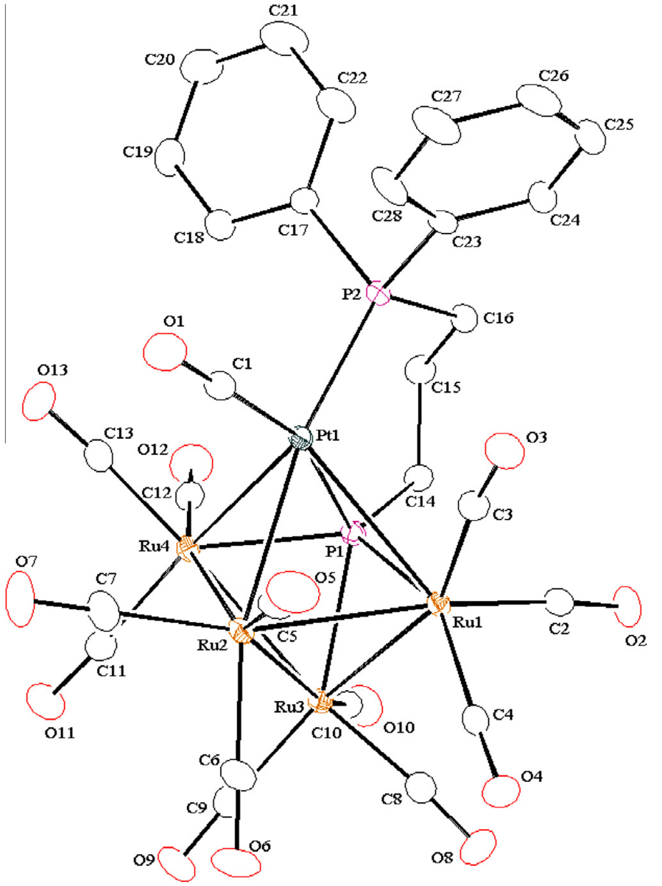

Fig. 2. ORTEP diagram of $Ru_4(CO)_{13}Pt(CO)(\mu_4\text{-}PCH_2CH_2CH_2PPh_2)$ (**5a**) with ellipsoidal model of probability level = 40%. All H are omitted. Selected bond distances (Å) and angles (°): Pt(1)–C(1) 1.882(4); Pt(1)–P(1) 2.3015(10); Pt(1)–P(2) 2.3196(10); Ru(1)–P(1) 2.4179(10); Ru(3)–P(1) 2.3537(10); Ru(4)–P(1) 2.3784(10); Pt(1)–Ru(2) 2.7452(3); Pt(1)–Ru(4) 2.8769(3); Pt(1)–Ru(1) 2.9122(3); Ru(1)–Ru(2) 2.7823(4); C(1)–Pt(1)–P(1) 161.27(13); C(14)–P(1)–Pt(1) 120.32(12); C(1)–Pt(1)–P(2) 99.81(12); P(1)–Pt(1)–P(2) 96.75(3); C(1)–Pt(1)–Ru(2) 87.92(12); P(1)–Pt(1)–Ru(2) 77.01(2); P(2)–Pt(1)–Ru(2) 168.96(3); C(1)–Pt(1)–Ru(4) 109.61(13); P(1)–Pt(1)–Ru(4) 53.29(3).

approximately cis arrangement of the two phosphorus ligands on the platinum, while the carbonyl is directed away from the phosphinidene. The Ru–Ru and Ru–Pt bond lengths fall within the range 2.7823(4)–2.8755(4) Å. Careful examination of these bond lengths reveals a distortion of the apical Ru(3) atom away from the center of the square. The metal–phosphinidene phosphorus bond lengths also show a distortion. All the Ru–P distances to the phosphinidene ligand are unsymmetrical and in this case one distance, P(1)–Ru(1) [2.4179(10) Å] is long compared to the others [P(1)–Pt = 2.3015 (10) Å, P(1)–Ru(3) = 2.3537(10) Å, P(1)–Ru(4) = 2.3784(10) Å].

The P(1)–C bond distance in the carbophosphinidene ligand of 1.841(4) Å is comparable to those observed in other phosphinidene complexes [32] and longer than the P(2)–C bond distance. The Pt–P(2) distance of 2.3196(10) Å is a normal Pt–PPh$_2$ distance, longer than the P(1)–Pt bond, 2.3015(10) Å. The ^{31}P NMR spectrum of **5a** shows peaks at δ 408 and 13.2 for the phosphinidene and phosphine ligands, respectively. The two bond P–P coupling constant is 14 Hz. This small coupling constant reflects the relative cis arrangement of these two ligands on platinum. A ^{195}Pt coupling constant of 3126 Hz is observed in the satellites of the diphenylphosphino resonance, while the ^{195}Pt coupling to the phosphinidene phosphorus atom is much smaller, being 864 Hz.

The platinum–carbonyl interactions are almost linear [O(1)–C(1)–Pt(1) = 175.9(4)°]. The Ru–C–O angles [ranging from 171.0(3) to 179.2(4)°] are much closer to linearity, without any semi-bridging CO ligands. As well, the Ru–C distances [ranging from 1.895(4) to 1.927(5) Å] are slightly longer than the Pt–C distance [1.882(4) Å]. These parameters confirm that the platinum–carbonyl interactions are relatively strong and may suggest that the removal of electron density from the electron-rich Pt center is not easy. In solution, the infrared spectrum of **5a** also shows no evidence for bridging carbonyls, with the lowest frequency band occurring at 2013 cm^{-1}.

As the electronegativity of the group on phosphorus increases, the phosphorus chemical shift moves further downfield [32]. A parallel trend is observed in the phosphinidene phosphorus-platinum coupling constants, which increase as the electronegativity of the phosphorus substituent increases.

The mass spectrum of the isolated compound **5**, showed the step-wise CO dissociation pattern from the molecular ion (m/z = 1034.7) with the mass fragments corresponding to Pt(dppp)$^+$ (m/z = 607.4) and other species of lower mass (Fig. 3). A similar fragmentation pattern was observed in the dppe and PPh$_3$ analogues.

Relative energies of the intermediates on the potential energy surface are summarized in Fig. 4. Our calculations indicate that the proposed reaction mechanism for the formation of a platinum-ruthenium trinuclear cluster via a hexacoordinate Pt(IV) species is kinetically and thermodynamically feasible. The method used in these calculations show the overall reaction to be exothermic by 79.8 kcal/mol, while the alkenyl dissociation energy from (V) to (VI) is exothermic by 45.5 kcal/mol. The rate-determining step appears to be the isomerization of the terminal ω-alkenyl to the internal alkenyl complex via the ruthenium–hydride(III). The optimized geometries of (II) and (IV) do not show any agostic interaction between the ruthenium center and the allylic protons or C$_\alpha$ protons respectively.

3.2. Transformations of the PPh$_3$ derivatives

In CH$_2$Cl$_2$ solution, compound **7** undergoes a slow and irreversible transformation reaction Eq. (1) in air or under UV light at room temperature within a few hours to give the known product **13** [4] in a reasonable yield (36%). During this reaction the {PtRu$_2$} framework of **7** is been completely changed into a cluster with a {Pt$_2$Ru} core (**13**) and Ru$_3$(CO)$_{11}$(PPh$_3$). It was found that this transformation reaction Eq. (1) was selective to the PPh$_3$ derivatives of the {PtRu$_2$} clusters and was not observed with the dppp and dppe analogues **5** and **6**. Compound **13** was characterized by a combination of IR, ^{1}H and ^{31}P NMR spectroscopy, and single crystal X-ray diffraction analysis. The ORTEP diagram of the

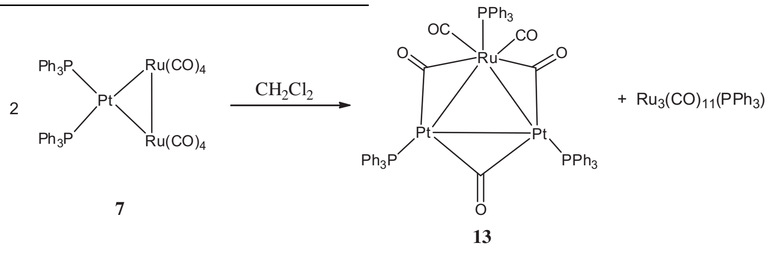

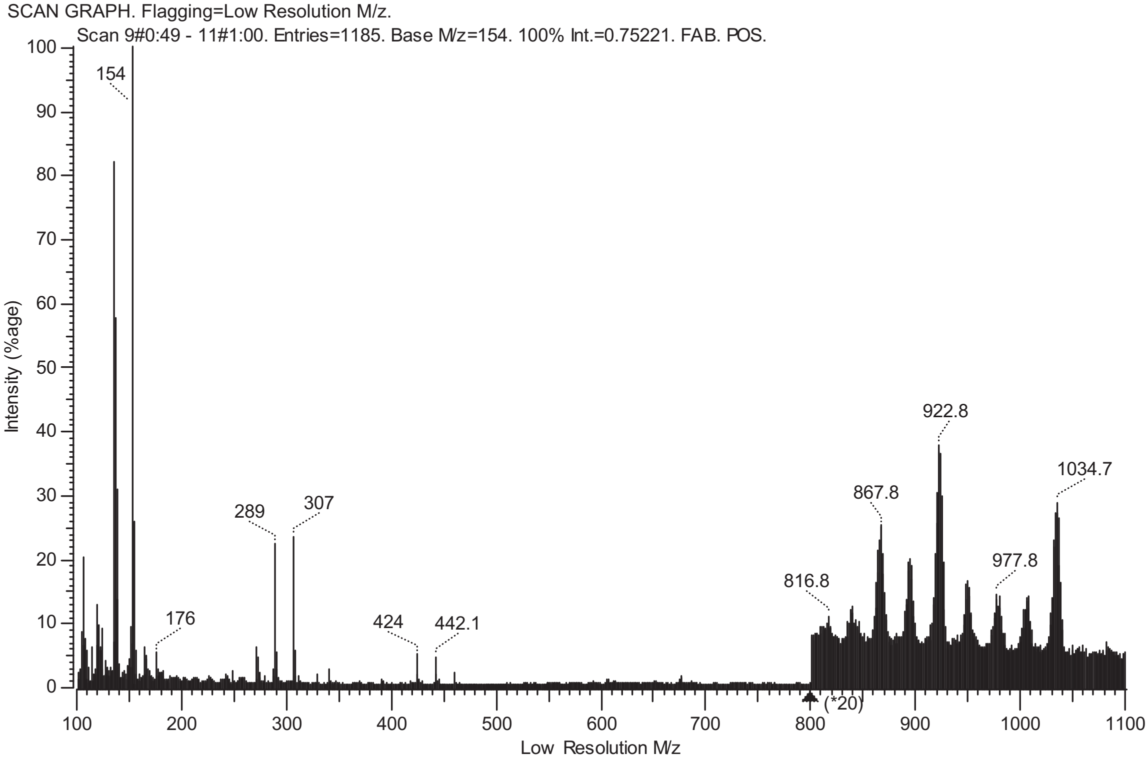

Fig. 3. Mass spectra of **5** showing the step-wise 'CO' dissociation pattern from the molecular ion (m/z = 1034.7).

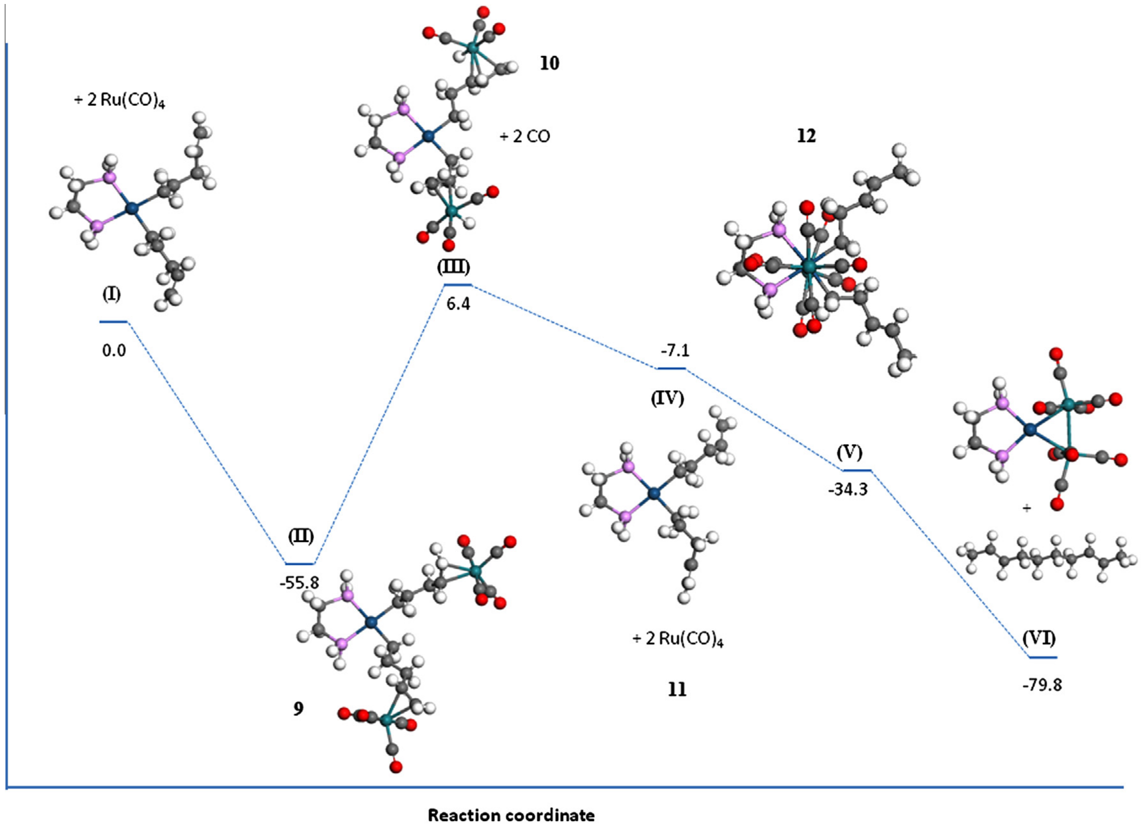

Fig. 4. Energy profile for proposed intermediates and transition states in the reaction mechanism. The relative energies are given in kcal/mol.

molecular structure **13** is shown in Fig. 5. The crystallographic data was collected at 113 K which generated better refinement with more precise molecular parameters, as compared to the same structure of **13** previously reported by Bruce et al. [4]. The structure of **13** is isostructural with the osmium analogue of the type {$PtOs_2$} [4] and consists of a triangular array of two platinum atoms and one ruthenium atom. There are two terminal carbonyl ligands bonded to each Ru atom and three carbonyls are bridging along the three metal–metal edges. The Pt(1)–P(1) and Pt(2)–P(2) bond lengths of 2.263(2) and 2.270(6) Å, respectively, are similar in distance and are in the range of usual Pt–P bond distances (2.26–2.28 Å) [33]. The presence of the bridging CO ligands across the Ru–Pt bonds does not influence the Pt–P bond distances.

3.3. Reaction of dppm derivatives

In contrast to the dppp and dppe analogues, the reaction of [Pt(dppm)(ω-pentenyl)$_2$] (**8**) with [$Ru_3(CO)_{12}$] yielded a known dppm bridging complex, [$PtRu_2(CO)_6(\mu\text{-dppm})_2$] (**14**) [34], as shown Scheme 3. The ^{31}P NMR spectrum of complex **14** shows two resonances at δ 16.8 (d) for the less shielded Ru bonded P and at δ 8.3 (d) for the more shielded Pt bonded P, with equal intensities. The benzene solvated crystal structure of **14** is shown in Fig. 6. The platinum atom and the two ruthenium atoms form a triangular structure. Two dppm ligands bridge both Pt–Ru metal–metal edges, but not along the Ru–Ru vector. All six carbonyl ligands are terminal and are found to coordinate selectively to the two ruthenium atoms in the cluster. It is clearly evident from the packing diagram that the two molecules of benzene in the crystal lattice do not show any disorder or molecular interactions with the structure of the cluster. Further, characterization data of compound **14** are in agreement with the literature values [34].

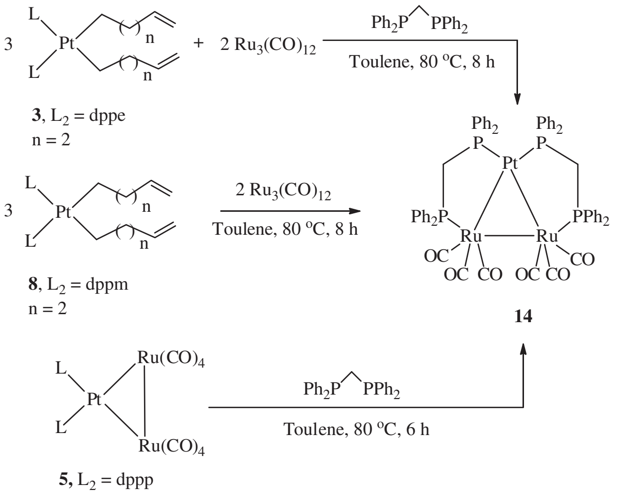

Scheme 3.

Attempts to make a mixed ligand trinuclear complex, substituting the dppp ligand by dppm, were not successful as the same product **14** was obtained when a $CHCl_3$ solution of **5** was refluxed with dppm (Scheme 3).

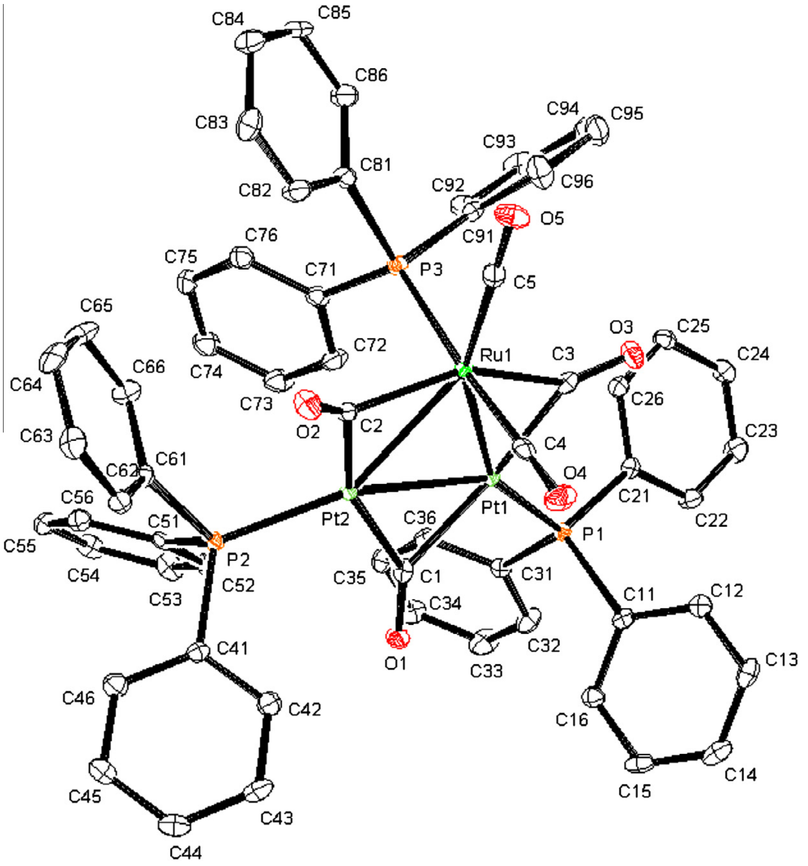

Fig. 5. Molecular structure of **13** (ORTEP diagram; 40% probability ellipsoids). Hydrogen atoms are omitted for clarity. Selected bond lengths (Å): Pt(1)–P(1) 2.269(6); Pt(2)–P(2) 2.270(6); Ru(1)–P(1) 2.437(5); Pt(1)–Ru(1) 2.734(1); Pt(2)–Ru(1) 2.741(2); Ru–CO(4) 1.889(11); Ru–CO(2) 1.900(10).

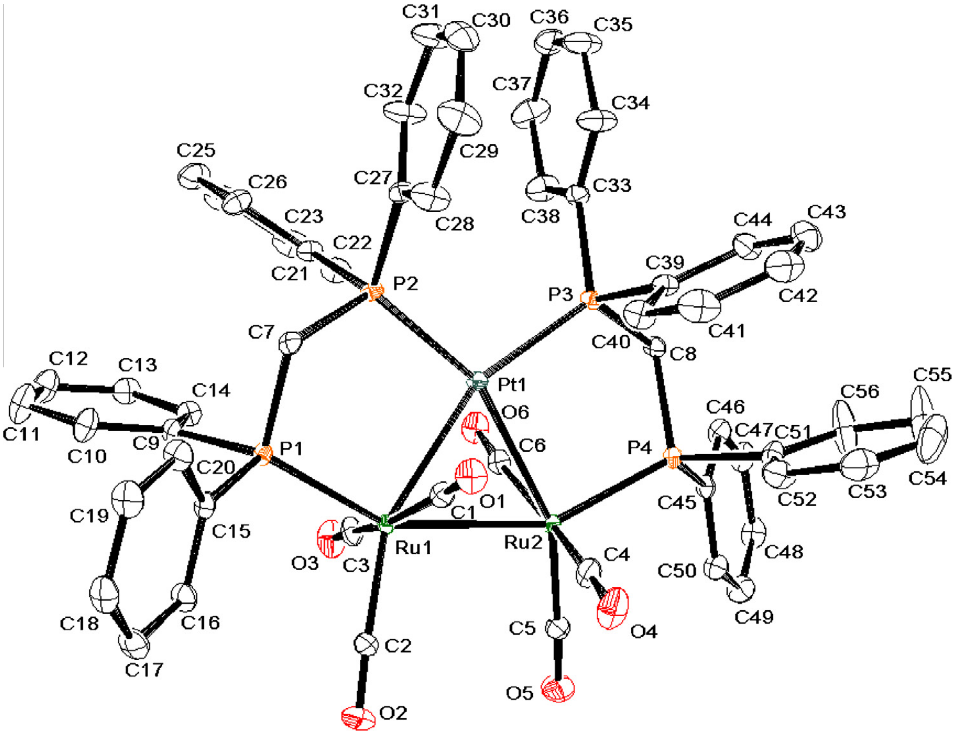

Fig. 6. Molecular structure of **14** (ORTEP diagram; 40% probability ellipsoids). Hydrogen atoms and two benzene molecules are omitted for clarity. Selected bond lengths (Å) and angles (°): Pt(1)–P(2) 2.2464(3); Pt(1)–P(3) 2.2536(3); Pt(1)–C(6) 2.5832(13); Pt(1)–Ru(1) 2.67272(15); Pt(1)–Ru(2) 2.67870(16); Ru(1)–Ru(2) 2.8486(2); Ru(2)–C(5) 1.8967(14); Ru(2)–C(6) 1.9113(13); Ru(2)–C(4) 1.9258(14); O(1)–C(1)–Ru(1) 174.26(11); O(6)–C(6)–Ru(2) 173.52(11); O(6)–C(6)–Pt(1) 113.26(10); Ru(2)–C(6)–Pt(1) 71.39(4).

4. Summary

A new route has been used to synthesize a series of platinum based mixed bimetallic carbonyl clusters from bis(1-alkenyl)Pt(II) compounds as precursors, and the unexpected synthesis of a substituted phosphinidene mixed metal cluster containing a quadruply bridging phosphorus atom was also achieved. The potential energy surface, optimized using density functional theory, is fully consistent with the postulated reaction mechanism and provides insight into the mechanisms by which the clusters are formed. Studies on the synthesis of novel carbonyl clusters of the type {$PtOs_2$}, {$PtFe_2$}, {$NiRu_2$} and {$NiFe_2$} are underway.

Acknowledgements

Dr. ASRK is highly grateful to Council of Scientific and Industrial Research India (CSIR-INDIA) for the financial support of this work through research grants Ref. No. 01(2541)/11/EMR-II. Also we thank Dr. M.W. Day (California Institute of Technology, California) for the X-ray structural data of compound **13**. Mr. Sadhana Venkatesh is grateful to CSIR for the fellowship to carry out the proposed research work. Dr. ASRK and his group members thank DST-VIT-FIST for NMR and SAIF-VIT Universiy for other instrumentation facilities.

References

[1] (a) S. Hermans, R. Raja, J.M. Thomas, B.F.G. Johnson, G. Sankar, D. Gleeson, Angew. Chem., Int. Ed. Engl. 7 (2001) 1211;
(b) D.S. Shephard, T. Maschmeyer, G. Sankar, J.M. Thomas, D. Ozkaya, B.F.G. Johnson, R. Raja, R.D. Oldroyd, R.G. Bell, Chem. Eur. J. 7 (1998) 1214.
[2] T. Khimyak, B.F.G. Johnson, J. Cluster Sci. 15 (2004) 543.
[3] A. Sivaramakrishna, B.C.E. Makhubela, H.S. Clayton, J.R. Moss, Coord. Chem. Rev. 252 (2008) 1460.
[4] (a) M.I. Bruce, J.G. Matisons, B.W. Skelton, A.H. White, Aust. J. Chem. 35 (1982) 687;
(b) M.I. Bruce, M.R. Snow, E.R.T. Tiekink, Aust. J. Chem. 39 (1986) 2145.
[5] R.D. Adams, G. Chen, J.G. Wang, W. Wu, Organometallics 9 (1990) 1339.
[6] (a) A.J. Dent, L.J. Farrugia, A.G. Orpen, S.E. Stratford, J. Chem. Soc., Chem. Commun. (1992) 1456;
(b) L.J. Farrugia, N. MacDonald, R.D. Peacock, J. Chem. Soc., Chem. Commun. (1991) 163;
(c) R.D. Adams, B. Captain, W. Fu, P.J. Pellechion, Chem. Commun. (2000) 937.
[7] (a) R.D. Adams, M.P. Pompeo, W. Wu, Inorg. Chem. 30 (1991) 2899;
(b) R.D. Adams, M.S. Alexander, I. Arafa, W. Wu, Inorg. Chem. 30 (1971) 4717.
[8] S. Hermans, J. Sloan, D.S. Shephard, B.F.G. Johnson, L.H. Malcolm, Chem. Commun. 22 (2002) 276.
[9] J. Jia, J. Shen, L. Lin, Z. Xu, T. Zhang, D. Liang, J. Catal. 138 (1999) 177.
[10] (a) H. Liu, C. Song, L. Zhang, J. Zhang, H. Wang, D.P. Wilkinson, J. Power Sources 155 (2006) 95;
(b) B.L. Garcia, B. Captain, R.D. Adams, A.B. Hungria, P.A. Midgley, S.J.M. Thomas, J.W. Weidner, J. Cluster Sci. 18 (2007) 121.
[11] (a) J.M. Thomas, B.F.G. Johnson, R. Raja, G. Sankar, P.A. Modgley, Acc. Chem. Res. 36 (2003) 20;
(b) R. Raja, T. Khimyak, J.M. Thomas, S. Hermans, B.F.G. Johnson, Angew. Chem., Int. Ed. Engl. 22 (2001) 4638;
(c) R. Raja, G. Sankar, S. Hermans, D.S. Shephard, S. Bromley, J.M. Thomas, B.F.G. Johnson, T. Maschmeyer, Chem. Commun. 16 (1999) 1571.
[12] (a) A. Sivaramakrishna, H. Clayton, C. Kaschula, J.R. Moss, Coord. Chem. Rev. 251 (2007) 1294;
(b) K. Dralle, N.L. Jaffa, T.L. Roex, J.R. Moss, S. Travis, N.D. Watermeyer, A. Sivaramakrishna, Chem. Commun. (2005) 3865;
(c) A. Sivaramakrishna, H. Su, J.R. Moss, Angew. Chem., Int. Ed. Engl. 46 (2007) 3541;
(d) T. Mahamo, F. Zheng, A. Sivaramakrishna, G.S. Smith, J.R. Moss, J. Organomet. Chem. 693 (2008) 103;
(e) A. Sivaramakrishna, H. Su, J.R. Moss, Dalton Trans. (2008) 2228;
(f) F. Zheng, A. Sivaramakrishna, J.R. Moss, Inorg. Chim. Acta 361 (2008) 2871;
(g) A. Sivaramakrishna, H. Su, J.R. Moss, Organometallics 26 (2007) 5786;
(h) A. Sivaramakrishna, B.C.E. Makhubela, F. Zheng, H. Su, J.R. Moss, Polyhedron 27 (2008) 44;
(i) A. Sivaramakrishna, B.C.E. Makhubela, G.S. Smith, J.R. Moss, J. Organomet. Chem. 695 (2010) 1627;
(j) A. Sivaramakrishna, J.R. Moss, H. Su, Inorg. Chim. Acta 363 (2010) 3345.
[13] H.C. Clark, L.E. Manzer, J. Organomet. Chem. 59 (1973) 411.
[14] Z. Otwinowski, W. Minor, in: C.W. Carter, Jr, R,M. Sweet, Methods in Enzymology, Macromolecular Crystallography, Part A, vol. 276, Academic Press, 1997, p. 307.

[15] (a) G.M. Sheldrick, SHELXL-97 and SHELXS-97, University of Gottingen, Germany, 1997; (b) G.M. Sheldrick, SADABS, Multi-scan Absorption Correction Program for Area Detector Data, University of Gottingen, Germany, 1996.

[16] L.J. Barbour, J. Supramol. Chem. 1 (2001) 189.

[17] (a) B. Delley, J. Chem. Phys. 113 (2000) 7756;
(b) B. Delley, J. Chem. Phys. 92 (1990) 508.

[18] J.P. Perdew, Y. Wang, Phys. Rev. B 45 (1992) 13244.

[19] N.A. Benedek, I.K. Snook, K. Latham, I.J. Yarovsky, Chem. Phys. 122 (2005) 144102.

[20] H. Orita, Y. Inada, J. Phys. Chem. B 109 (2005) 22469.

[21] M. Jordan, H.C.M. Vosloo, Mol. Simul. 34 (2008) 997.

[22] (a) R.D. Adams, B. Captain, W. Fu, J.L. Smith, M.D. Smith, Organometallics 23 (2004) 589;
M.I. Bruce, G. Shaw, F.G.A. Stone, J. Chem. Soc., Dalton Trans. (1972) 1781.

[23] (a) P. Braunstein, J. Dehand, J.F. Nennig, J. Organomet. Chem. 92 (1975) 117;
(b) J. Fischer, A. Mitschler, R. Weiss, J. Dehand, J.F. Nennig, J. Organomet. Chem. 91 (1975) 37.

[24] L.J. Farrugia, J.A.K. Howard, P. Mitrprachachon, J.L. Spencer, F.G.A. Stone, P. Woodward, Chem. Commun. (1978) 260.

[25] R.D. Adams, B. Captain, L. Zhu, Inorg. Chem. 45 (2006) 430.

[26] R.D. Adams, B. Captain, W. Fu, Organometallics 25 (2006) 2049.

[27] R.D. Adams, W. Wu, Organometallics 12 (1993) 1248.

[28] L.J. Farrugia, in: F.G.A. Stone (Ed.), Advances in Organometallic Chemistry, vol. 31, Academic Press, California, p. 363.

[29] W.R. Hastings, M.R. Roussel, M.C. Baird, J. Chem. Soc., Dalton Trans. (1990) 203.

[30] (a) M. Bianchi, F. Piacenti, P. Frediani, U. Matteoli, J. Organomet. Chem. 135 (1977) 387;
(b) B. Fontal, M. Reyes, T. Suarez, F. Bellandi, N. Ruiz, J. Mol. Catal. A: Chem. 149 (1999) 87;
(c) F. Piacenti, M. Bianchi, P. Frediani, G. Menchi, U. Matteoli, J. Organomet. Chem. 417 (1991) 77;
(d) J.P. Collman, L.S. Hegedus, J.R. Norton, R.G. Finke, Principles and Applications of Organotransition Metal Chemistry, University Science Books, Mill Valley, CA, 1987. p. 527.

[31] A. Sivaramakrishna, P. Mushonga, I.L. Rogers, F. Zheng, E. Nordlander, R.J. Haines, J.R. Moss, Polyhedron 27 (2008) 1911.

[32] (a) W. Wang, G.D. Enright, A.J. Carty, J. Am. Chem. Soc. 119 (2000) 12370;
(b) J.H. Yamamoto, K.A. Udachin, G.D. Enright, A.J. Carty, Chem. Commun. (1998) 2259;
(c) J.F. Halet, R. Hoffmann, J.Y. Saillard, Inorg. Chem. 24 (1985) 1695.

[33] F.H. Allen, O. Kennard, D.G. Watson, R.Taylor, in: A.J.C. Wilson (Ed.), International Tables of Crystallography, vol. C, Kluwer Academic Publishers, Dordrecht, 1992.

[34] B.T. Sterenberg, M.C. Jennings, R.J. Puddephatt, Organometallics 18 (1999) 2162.